Functional Networks Analysis and a bit more

J. Kurths[1 2 3], J. Donges, R. Donner, N. Marwan, S. Schinkel, W. Sommer,G. Zamora and Y. Zou

[1]Potsdam Institute for Climate Impact Research, RD Transdisciplinary Concepts and Methods

[2] Inst. of Physics, Humboldt University Berlin

[3] University of Aberdeen, King´s College

http://www.pik-potsdam.de/members/kurths/

juergen.kurths@pik-potsdam.de

Contens

- Introduction
- Network of networks and brain functionality
- Recurrence and recurrence networks
- Application to Paleoclimate
- Conclusions

Network of Networks

Interconnected Networks

Interdependent Networks

Transportation Networks

- Romans built > 850.000 km roads (Network)
- „Silk Street“

  (Network)

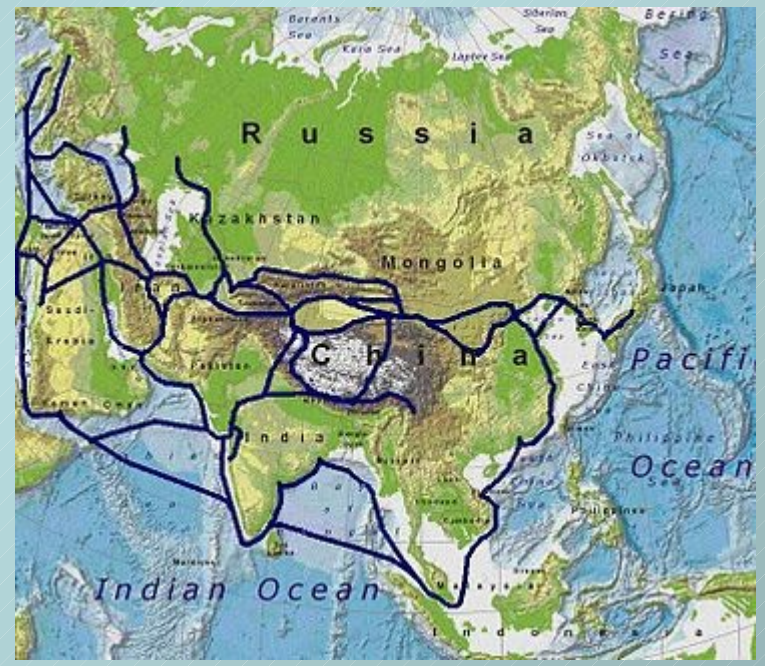

Papenburg: Monster Black-Out 06-11-2006

- Meyer Werft in Papenburg
- Newly built ship Norwegian Pearl

  length: 294 m, width: 33 m
- Cut one line of the power grid
- Black-out in

  Germany (> 10 Mio people)

  France (5 Mio people)

  Austria, Belgium, Italy, Spain

Application: Brain Dynamics

Concept: network of networks

(anatomy vs. functionality)

Frontiers Neurosc. 5, 83, (2011)

Frontiers Neuroinform. 4, 1 (2010)

Phys Rev Lett 97, 238103 (2006)

System Brain: Cat Cerebal Cortex

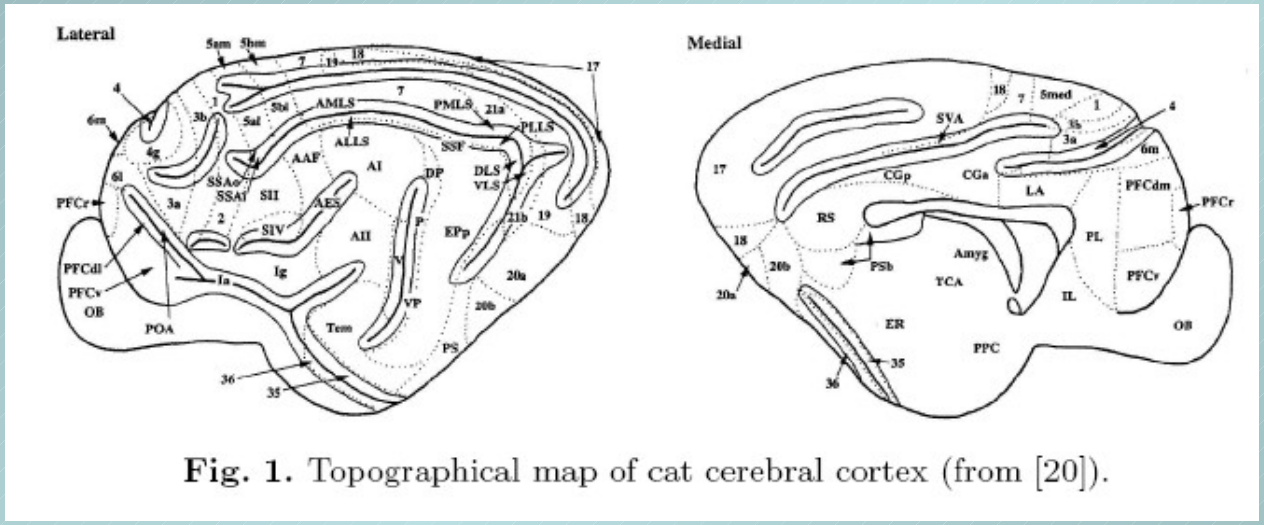

Fig. 1. Topographical map of cat cerebral cortex (from [20]).

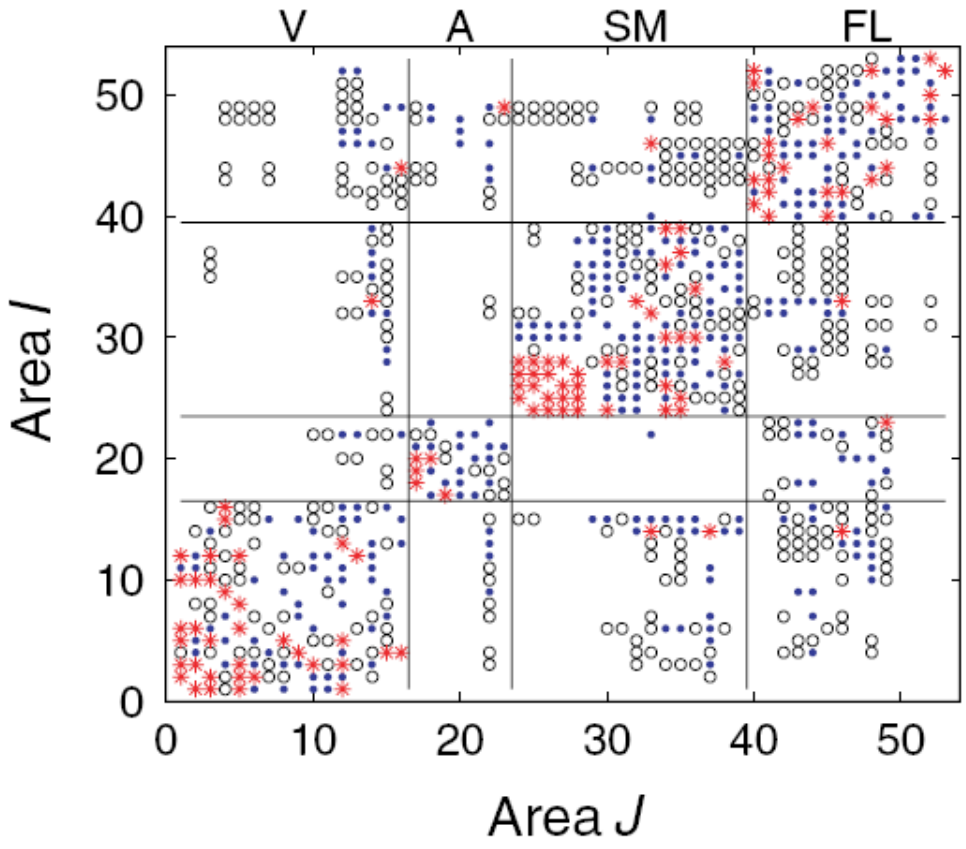

Density of connections between the four com-munities

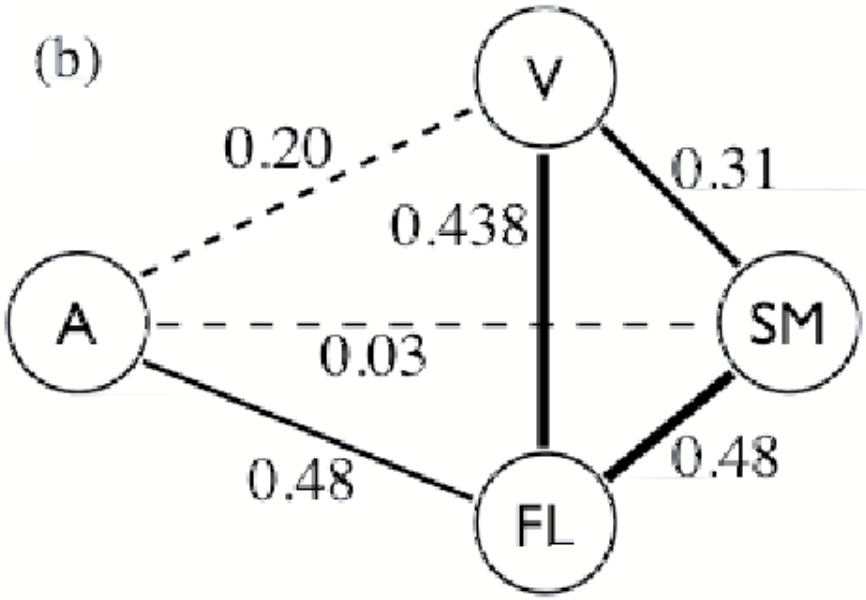

- Connections among the nodes: 2 … 35
- 830 connections
- Mean degree: 15

Betweenness

Betweenness Centrality B

Number of shortest paths that connect nodes j and k n_{jk}

Number of shortest paths that connect nodes j and k AND path through node i $n_{jk}(i)$

Local betweenness of node i

$$b_i = \sum_{j,k,j\neq k} \frac{n_{jk}(i)}{n_{jk}}$$

(local and global aspects included!)

Betweenness Centrality B = < b_i >

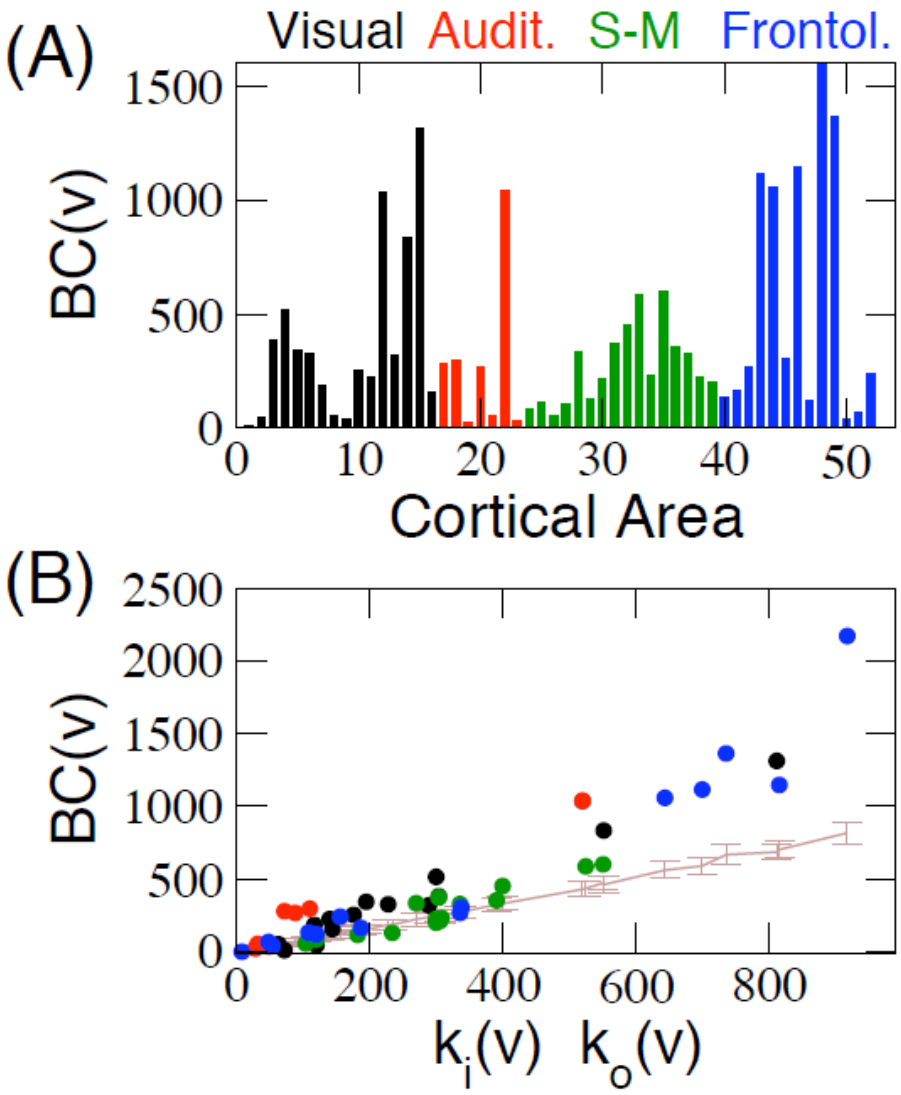

FIG. 4: Centrality of cortical areas. (**A**) Betweenness of cortical areas shows that at each sensory system few areas are very central. (**B**) Comparison between BC of cortical areas and the expected centrality due to their degree (brown line). As a consequence of the modular and hierarchical organisation of the network, low degree areas closely follow the expected centrality, but hubs are significantly more central than expected. Communication paths between sensory systems are centralised through the hubs.

Major features of organization of cortical connectivity

- Large density of connections (many direct connections or very short paths – fast processing)
- Clustered organization into functional com- munities
- Highly connected hubs (integration of multisensory information)

Modelling

- Intention:

  Macroscopic ➔ Mesoscopic Modelling

Network of Networks

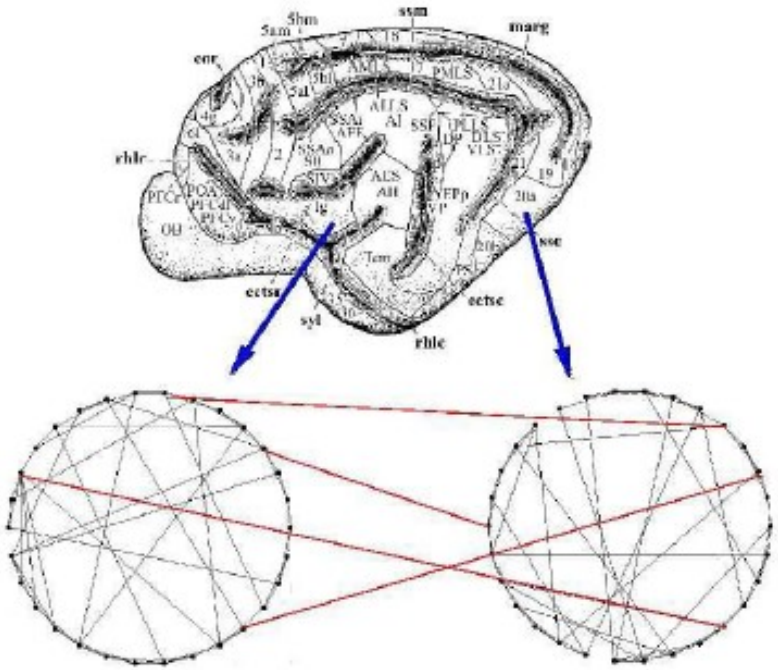

Fig. 3. The modeled system — a network of networks. Note that local subnetworks have small-world structure.

Model for neuron i in area I

$$\epsilon \dot{x}_{I,i} = f(x_{I,i}) + \frac{g_1}{k_a} \sum_{j}^{N_a} M_I^L(i,j)(x_{I,j} - x_{I,i})$$

$$+ \frac{g_2}{\langle w \rangle} \sum_{J}^{N} M^C(I,J) L_{I,J}(i)(\bar{x}_J - x_{I,i}),$$

$$\dot{y}_{I,i} = x_{I,i} + a_{I,i} + D\xi_{I,i}(t),$$

where

$$f(x_{I,i}) = x_{I,i} - \frac{x_{I,i}^3}{3} - y_{I,i}.$$

FitzHugh Nagumo model

Transition to synchronized firing

g – coupling strength – control parameter

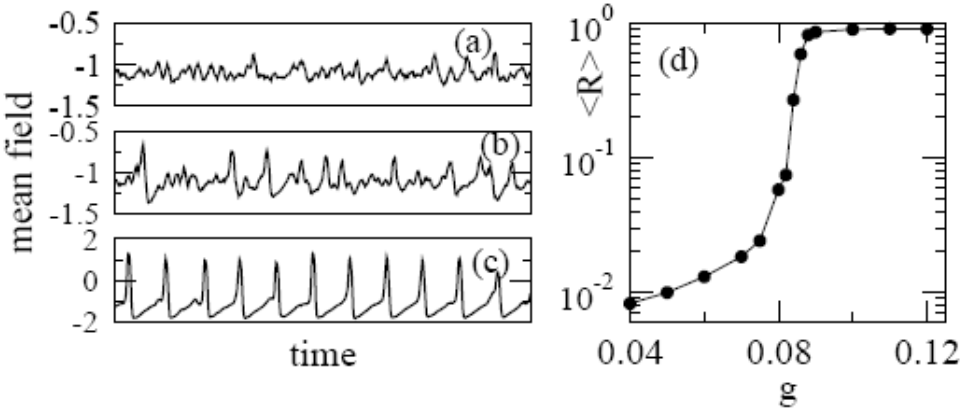

FIG. 2: Mean activity X of one area at various couplings (a) $g = 0.06$, (b) $g = 0.082$ (c) $g = 0.09$. The average correlation coefficient $\langle R \rangle = \frac{1}{N(N-1)} \sum_{I \neq J}^{N} R(I, J)$ $(N = 53)$ vs. g.

Possible interpretation: functioning of the brain near a 2nd order phase transition

Functional Organization vs. Structural (anatomical) Coupling

Formation of dynamical clusters

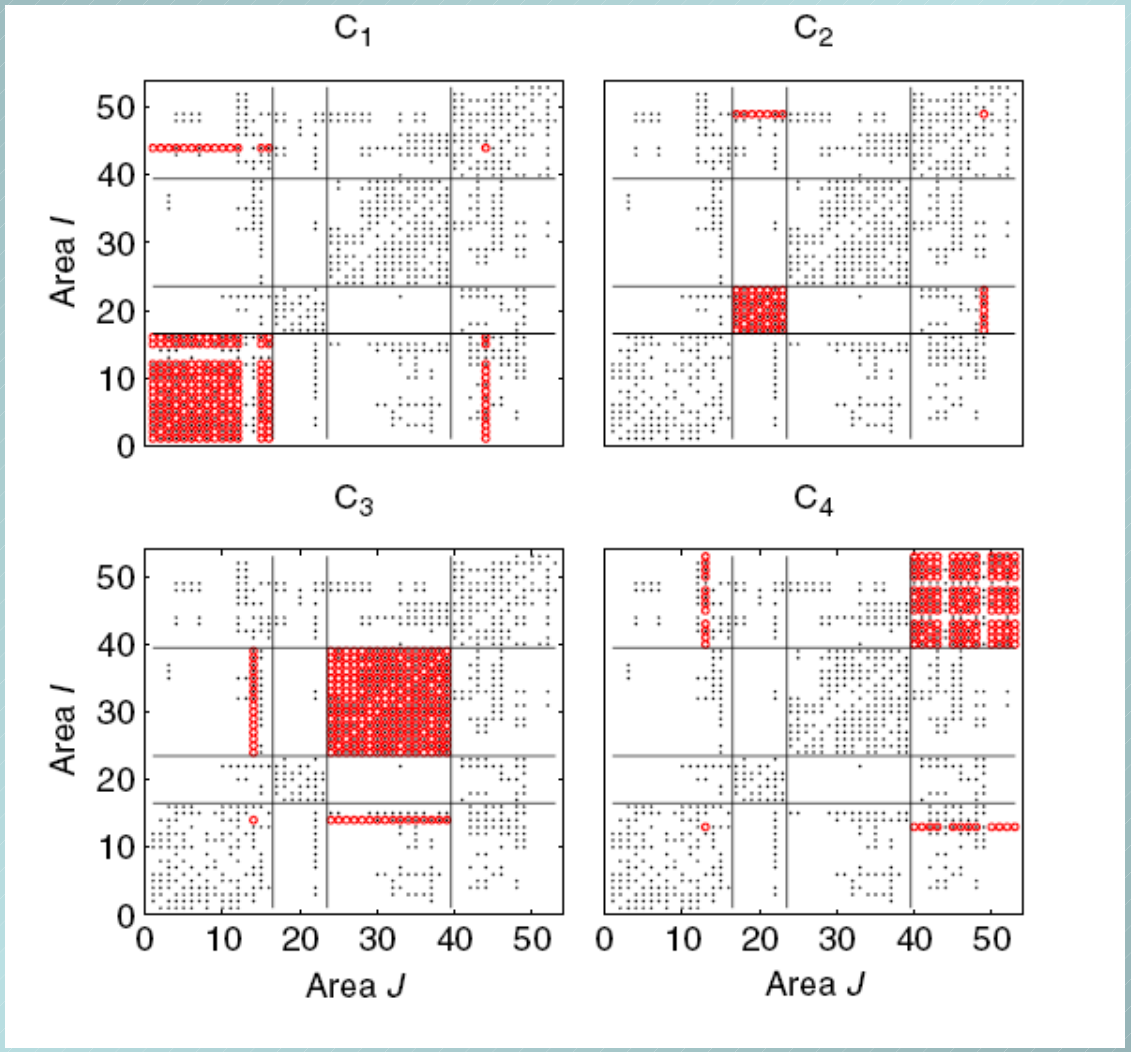

Cognitive Experiment

- Given two words:

  a) synonyms (primed condition) car - driver

  b) unrelated words (unprimed) sun - head
- ECG measurements of event-related potentials (126 electrodes)
- Analysis

  a) simple difference of potentials

  b) network synchronization analysis

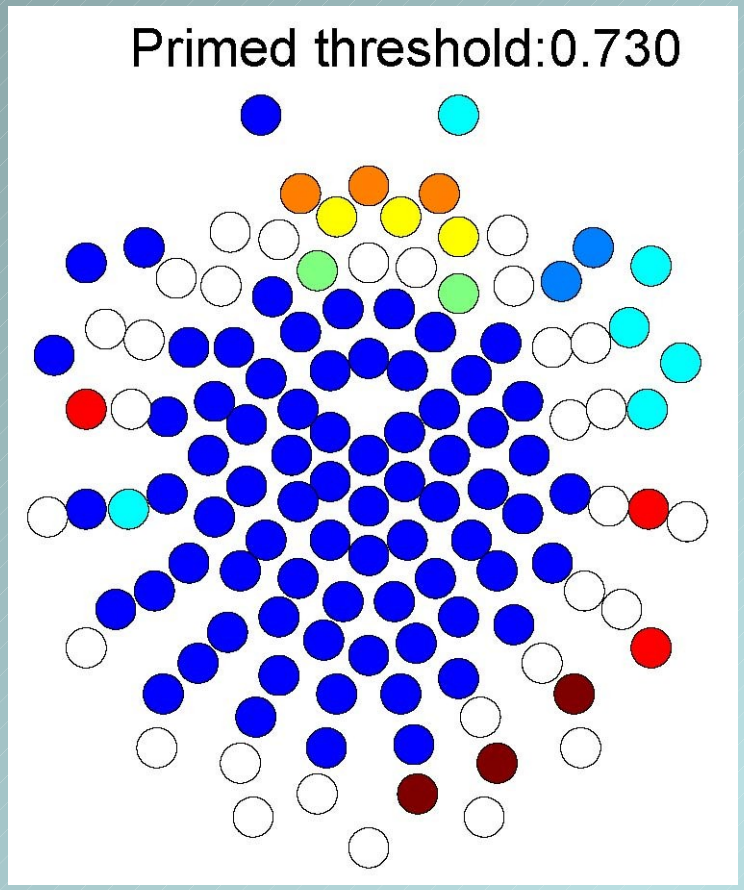

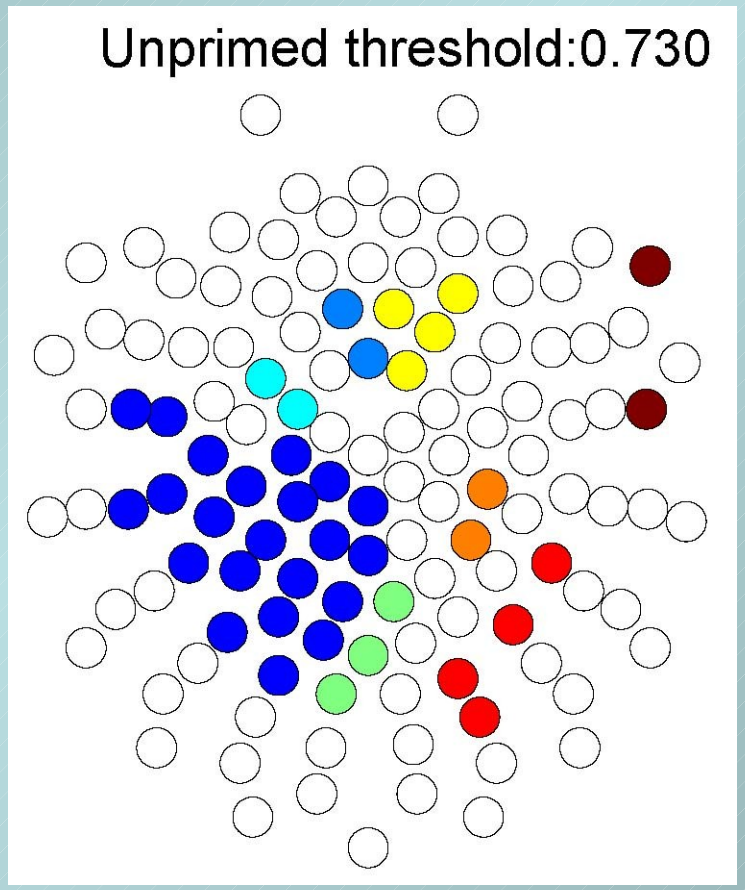

Global synchronization
(one color dominates)

vs.

Several network components

J. Neurosc. Meth., 2011

Recurrence Networks

Concept of Recurrence

Recurrence

Περιχωρεσιζ – perichoresis (Anaxagoras)

Concept of Recurrence

Recurrence theorem:

Suppose that a point P in phase space is covered by a conservative system. Then there will be trajectories which traverse a small surrounding of P infinitely often.
That is to say, in some future time the system will return arbitrarily close to its initial situation and will do so infinitely often.
(Poincare, 1885)

Recurrence – fundamental property of a dynamic system

How to elaborate?
How to quantify?

Recurrence plots

- **Recurrence plot**

  $R(i , j) = \Theta(\varepsilon - |x(i) – x(j)|)$

Θ – Heaviside function

ε – threshold for neighborhood (recurrence to it) - (Eckmann et al., 1987

Generalization for Data Analysis:

Statistical properties of all side diagonals and vertical elements

Recurrence-based Measures of Complexity

- Diagonal-line-based measures: determinism, longest diagonal line (Zbilut & Webber)

- Vertical-line-based measures: laminarity, trapping time

  (Phys Lett A, 2002, Phys Rev E, 2002)

Distribution of the Diagonals

$$P_\varepsilon(l) \approx \varepsilon^{D_2} \exp(-\tau K_2 l)$$

The following parameters can be estimated by means of RPs (Thiel, Romano, Kurths, CHAOS, 2004):

Correlation Entropy:

$$\hat{K}_2(\varepsilon, l) = \frac{1}{l\tau} \ln\left(\frac{1}{N^2} \sum_{s,t=1}^{N} \prod_{m=0}^{l-1} R_{t+m,s+m} \right)$$

Correlation Dimension:

$$\hat{D}_2(\varepsilon, l) = \ln\left(\frac{P_\varepsilon(l)}{P_{\varepsilon+\Delta\varepsilon}(l)} \right) \Big/ \left(\frac{\varepsilon}{\varepsilon + \Delta\varepsilon} \right)$$

Mutual Information:

$$\hat{I}_2(\varepsilon, \tau) = -2 \ln\left[\frac{1}{N^2} \sum_{i,j=1}^{N} R_{i,j} \right] + \ln\left[\frac{1}{N^2} \sum_{i,j=1}^{N} R_{i,j} R_{i+\tau, j+\tau} \right]$$

Example: logistic map

$$x(n+1) = r\, x(n)\, (1 - x(n))$$

Nonlinear difference equation

Parameter r

Supertrack function s (a)

$$s_{i+1}(a) = a\, s_i(a)(1 - s_i(a)), \quad s_0(a) = \tfrac{1}{2}, \quad i = 1, 2, \ldots$$

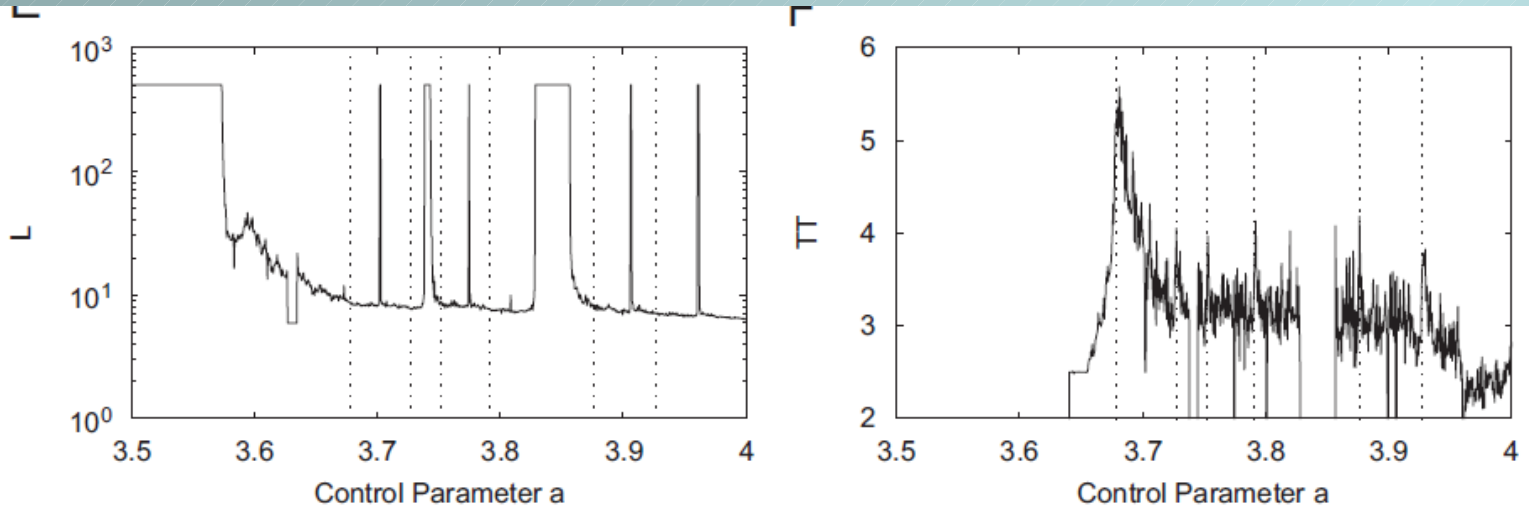

Fig. 24. Selected RQA measures *DET*, L_{max} and *L* and the measures *LAM*, V_{max} and *TT*. The vertical dotted lines indicate some of the points, at which band merging and laminar behaviour occur (cf. Fig. 22), whereby not all of them have been marked. Whereas (A) *DET*, (C) L_{max} and (E) *L* show periodic–chaos/chaos–periodic transitions (maxima), (B) *LAM*, (D) V_{max} and (F) *TT* exhibit in addition to those transitions (minima) chaos–chaos transitions (maxima). The differences between *LAM* and V_{max} are caused by the fact that *LAM* measures only the amount of laminar states, whereas V_{max} measures the maximal duration of the laminar states. Although some peaks of V_{max} and *TT* are not at the dotted lines, they correspond to laminar states (not all can be marked) [14].

Diagonal-based measures – identify regular-chaos transitions

Vertical-based measures – identify basic chaos-chaos transitions

Available online at www.sciencedirect.com
ScienceDirect
ELSEVIER
Physics Reports 438 (2007) 237–329
PHYSICS REPORTS
www.elsevier.com/locate/physrep

Recurrence plots for the analysis of complex systems

Norbert Marwan*, M. Carmen Romano, Marco Thiel, Jürgen Kurths

Nonlinear Dynamics Group, Institute of Physics, University of Potsdam, Potsdam 14415, Germany

Accepted 3 November 2006
Available online 12 January 2007
editor: I. Procaccia

Method of Recurrence Networks

combines:

1) recurrence properties of time series with
2) network characterization

Complex network approach for recurrence analysis

- Interprete a recurrence matrix obtained from a dynamical system as adjacency matrix and refer to a network with complex topology
- Elements are $A_{i,j} = R_{i,j} - \delta_{i,j}$
- Use of typical complex networks parameters: degree, betweennes, clustering

Phys. Lett. A 2009, New J. Phys. 2010

Transform of a periodic trajectory to a network

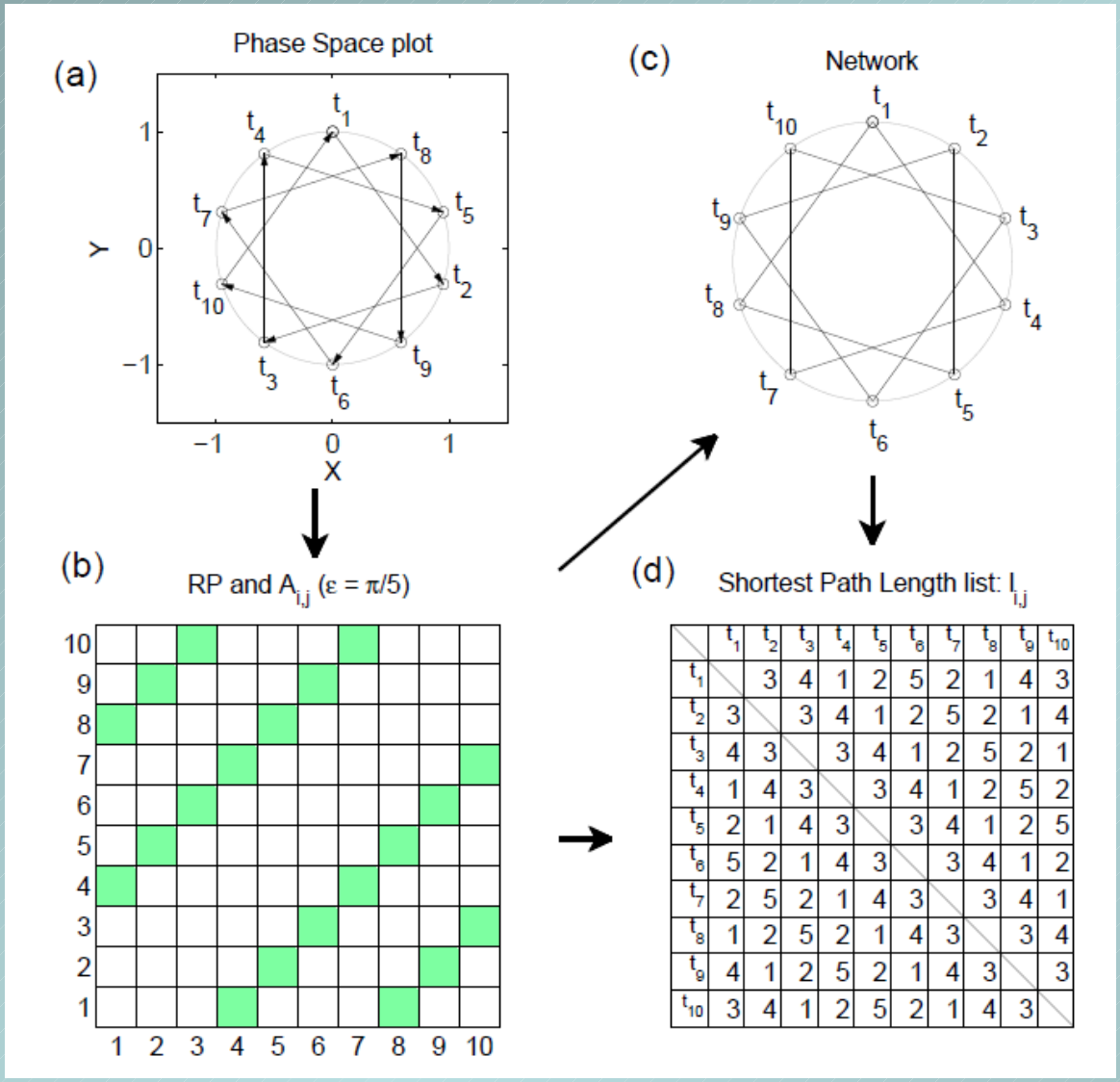

	t_1	t_2	t_3	t_4	t_5	t_6	t_7	t_8	t_9	t_{10}
t_1		3	4	1	2	5	2	1	4	3
t_2	3		3	4	1	2	5	2	1	4
t_3	4	3		3	4	1	2	5	2	1
t_4	1	4	3		3	4	1	2	5	2
t_5	2	1	4	3		3	4	1	2	5
t_6	5	2	1	4	3		3	4	1	2
t_7	2	5	2	1	4	3		3	4	1
t_8	1	2	5	2	1	4	3		3	4
t_9	4	1	2	5	2	1	4	3		3
t_{10}	3	4	1	2	5	2	1	4	3	

$$x(t) = \sin(6\pi \cdot 0.1t),\ y(t) = \cos(6\pi \cdot 0.1t)$$

$$\epsilon = \frac{\pi}{5}$$

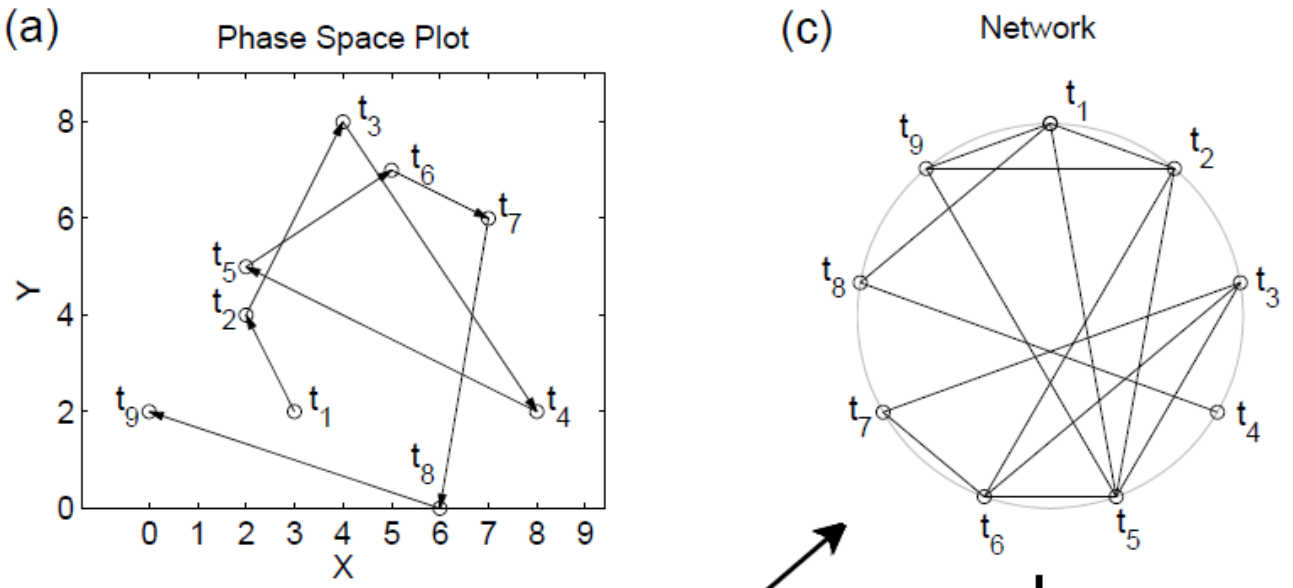

	t_1	t_2	t_3	t_4	t_5	t_6	t_7	t_8	t_9
t_1		1	2	2	1	2	3	1	1
t_2	1		2	3	1	1	2	2	1
t_3	2	2		4	1	1	1	3	2
t_4	2	3	4		3	4	5	1	3
t_5	1	1	1	3		1	2	2	1
t_6	2	1	1	4	1		1	3	2
t_7	3	2	1	5	2	1		4	3
t_8	1	2	3	1	2	3	4		2
t_9	1	1	2	3	1	2	3	2	

Non-periodic trajectory

Typical network parameters

- Degree centrality $$k_v = \sum_{i=1}^{N} A_{v,i}$$
- Link density $$\rho = \frac{1}{N(N-1)} \sum_{i,j=1}^{N} A_{i,j}$$
- Clustering Coefficient $$C_v = \frac{\sum_{i,j=1}^{N} A_{v,i} A_{i,j} A_{j,v}}{k_v (k_v - 1)}$$
- Average path length $$\mathcal{L} = \frac{1}{N(N-1)} \sum_{i,j=1}^{N} d_{i,j}$$

Logistic Map

Table 1
Control parameter, RQA and network measures for different dynamical regimes of the logistic map (RP parameter: $m = 1$, $\varepsilon = 0.05\sigma$).

Regime	a	L_{max}	LAM	$\mathcal{L}$	$\mathcal{C}$	ρ
Period-3	3.830	8996	0	1	1	0.333
Band merging	3.679	49	0.42	22.8	0.83	0.050
Laminar	3.791	39	0.12	23.3	0.79	0.040
Outer crisis	4.000	23	0.20	23.6	0.82	0.046

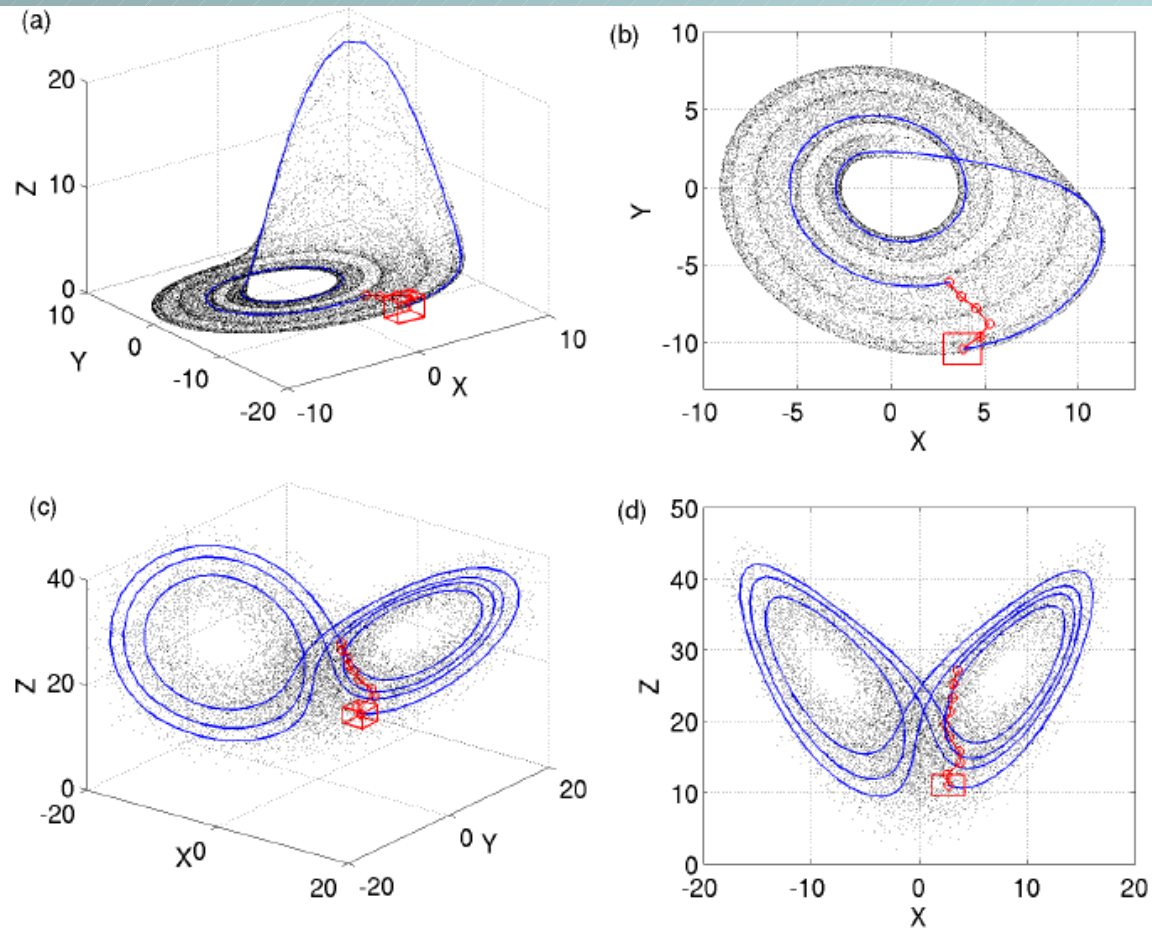

Figure 4. (a,b) Chaotic attractor of the Rössler system (dark dots) and realisation of one particular non-periodic trajectory (blue line), corresponding to $T = N\Delta t = 11.4$ time steps. The size of the considered neighbourhood $\epsilon = 1$ (maximum norm) is indicated by a red square around the initial condition. (Note that the square gives an idealised representation of the considered neighbourhood.) The red line displays the shortest path between the initial condition and the final value on this trajectory ($l = 5$). (c,d) One example trajectory of the Lorenz system with $T = 5$ time steps, and resulting shortest path between initial and final state ($\epsilon = 1.5$, $l = 9$).

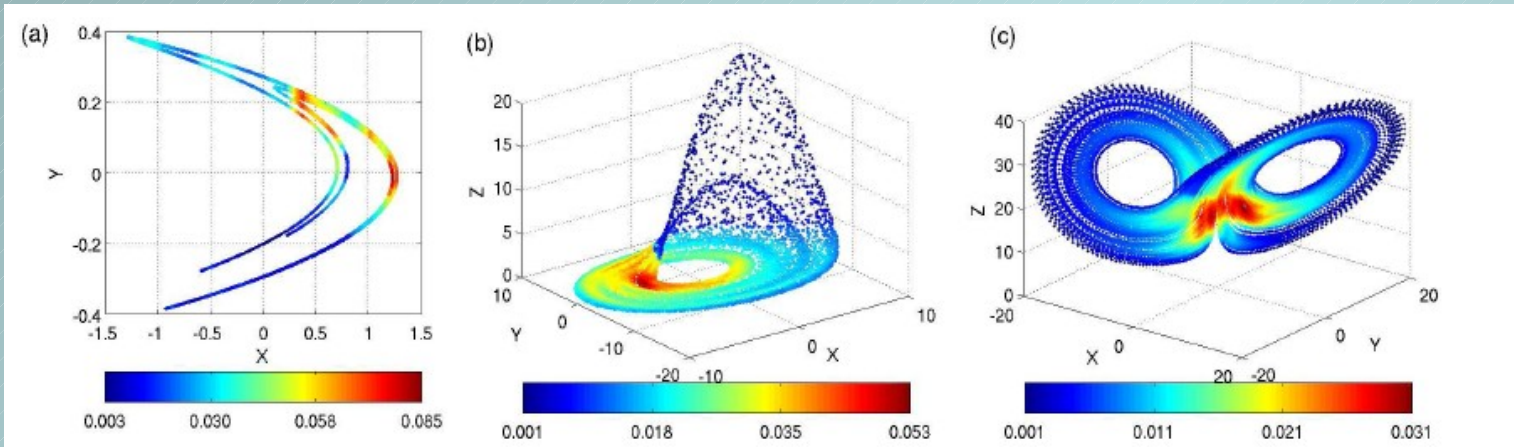

Figure 6. Colour-coded representation of the local recurrence rate RR_v (proportional to the degree centrality k_v) in phase space (a) Hénon map ($N = 10,000$), (b) Rössler ($N = 10,000$), and (c) Lorenz systems ($N = 20,000$). The value of ϵ for each case is chosen in such a way that the global recurrence rate $RR = \rho \approx 0.03$.

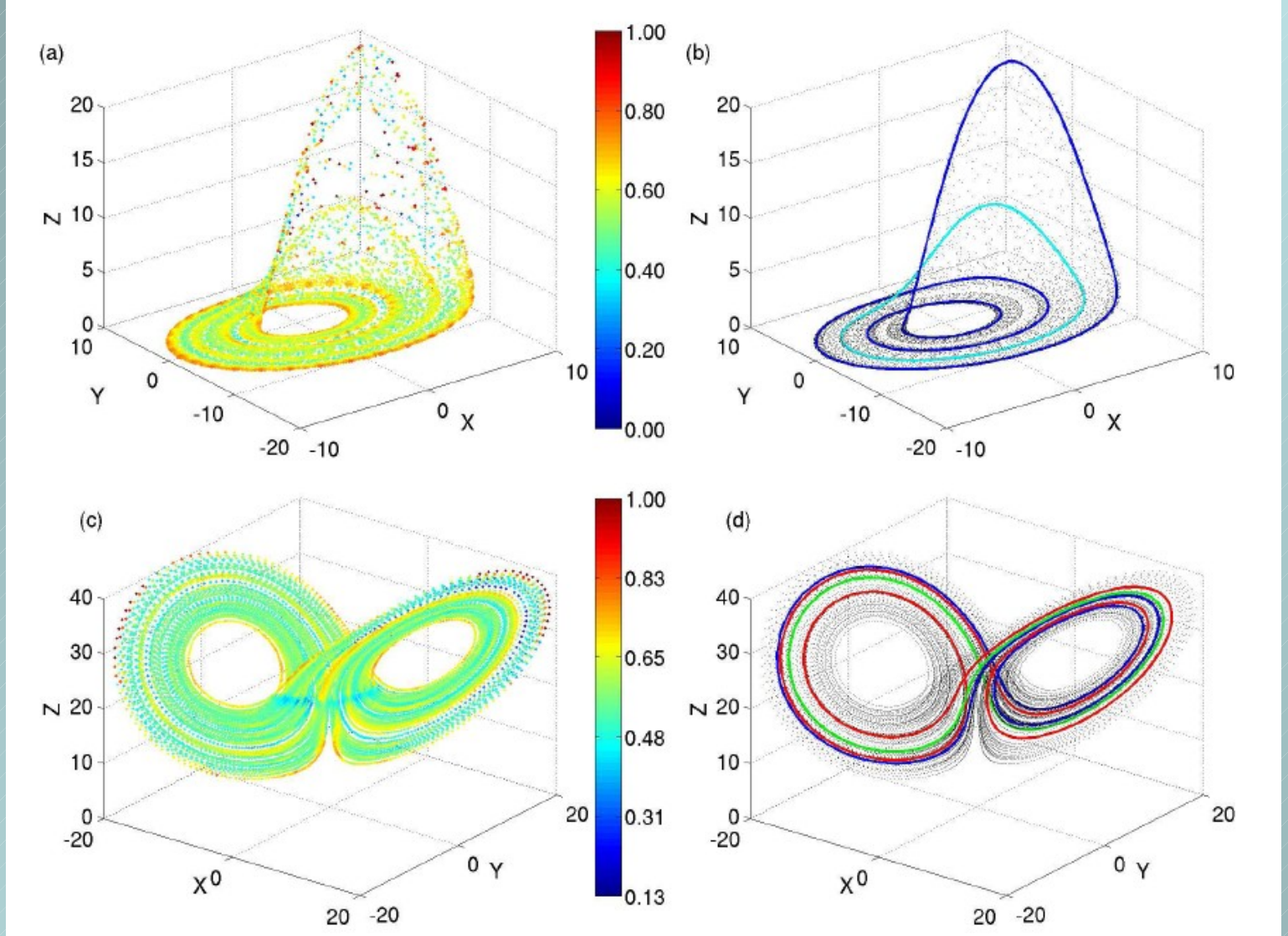

Figure 10. (a) Colour-coded representation of the local clustering coefficients C_v for the Rössler system ($N = 10,000$) in its phase space. (b) Several locations of the unstable periodic orbits with low periods, obtained using a method based on the windows of parallel lines in the corresponding recurrence plot as described in [9]. The chosen value of ϵ corresponds to a global recurrence rate of $RR = 0.01$. (c),(d) Same as (a),(b) for the Lorenz system ($N = 20,000$).

Estimation of these Parameters

- Crucial problem: select optimum recurrence threshold ε
- too large – boundary effects dominate
- too small – giant components break down

- Related to critical mean degree z_c (as percolation threshold)

Critical thresholds

- Critical recurrence threshold (PRE 2012)

$$\varepsilon_c(d) = \rho^{-1}\left(\frac{z_c(d)}{N-1}\right)$$

- Empirical critical mean degree (Dall et al., 2002)

$$z_c(d) = z_c(\infty) + Ad^{-\gamma}$$

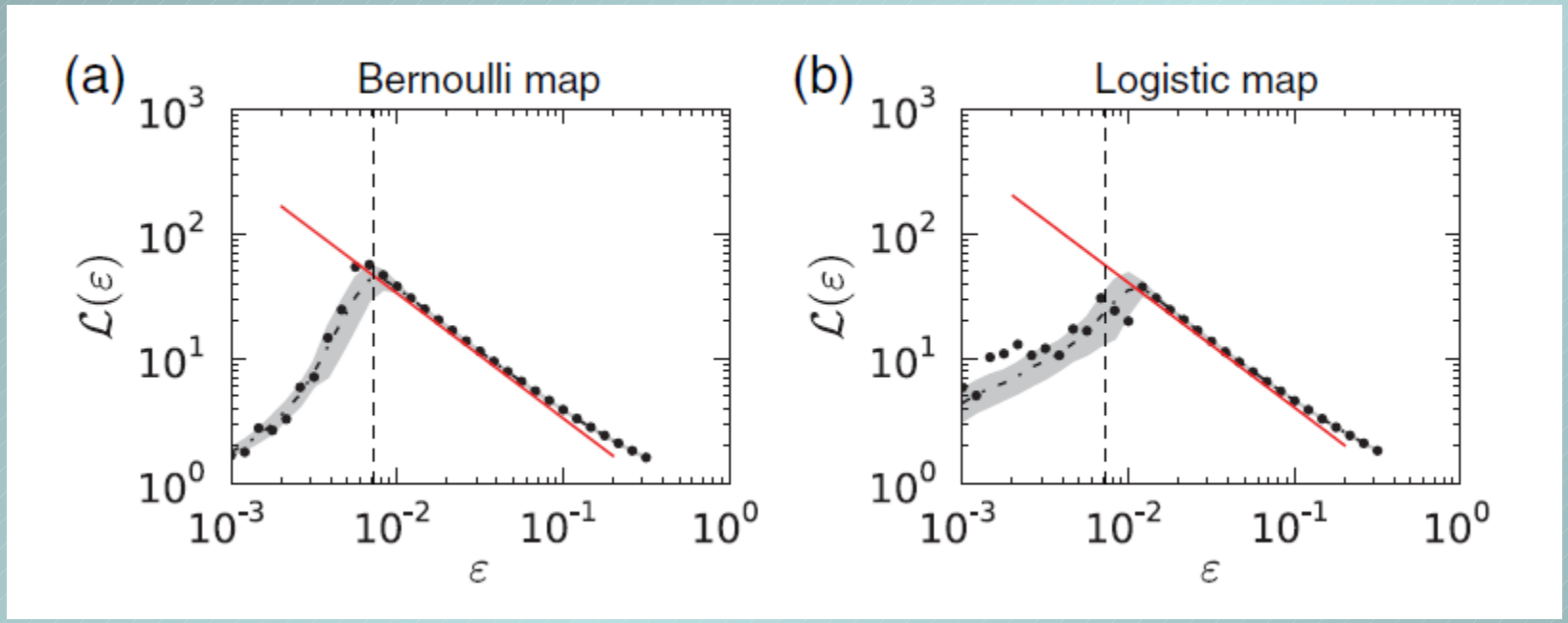

Continuous ε-average path length $\mathcal{L}(\varepsilon)$

System Earth

Natural vs. Anthropogenic Changes?

Looking into the Past - Palaeoclimatology

Palaeo-climate

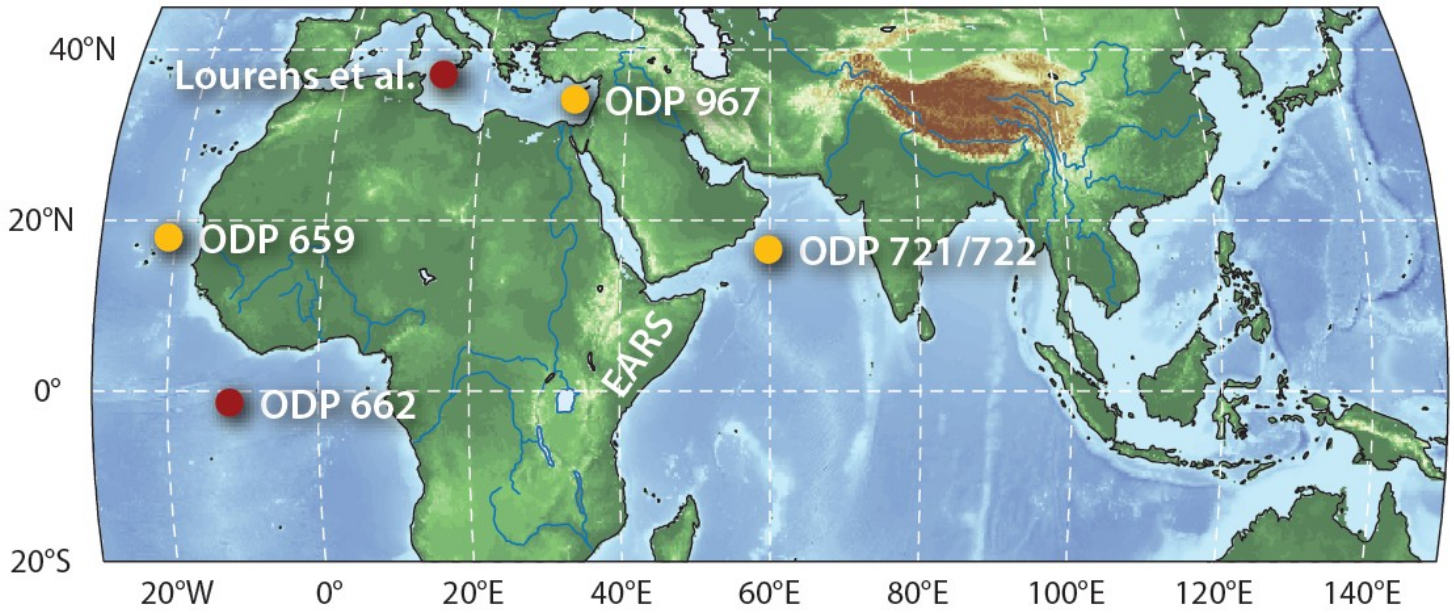

Fig. 1. Map displaying the locations of the marine sediment cores analyzed in this study (orange): ODP 659 (East Atlantic) (34), 721/722 (Arabian Sea) (1, 2), and 967 (Eastern Mediterranean Sea) (66). In addition, locations of additional complementary records of Plio-Pleistocene climate evolution (red) in the Atlantic (ODP site 662 (61)) and the Mediterranean (composite sequence of marine sediments at the Sicilian and Calabrian coast (69)) as well as the East African Rift System (EARS) are shown.

Palaeoclimatic Data

- Marine record from ocean drilling programme (ODP) in the atlantic, site 659
- Marine terrigenous dust measurements

➔epochs of arid continental climate in Africa

Record covers the last 4.5 Ma,

sampling = 4.1 ka, N = 1240

Terrigenous dust flux records site 659

and corresponding network measures

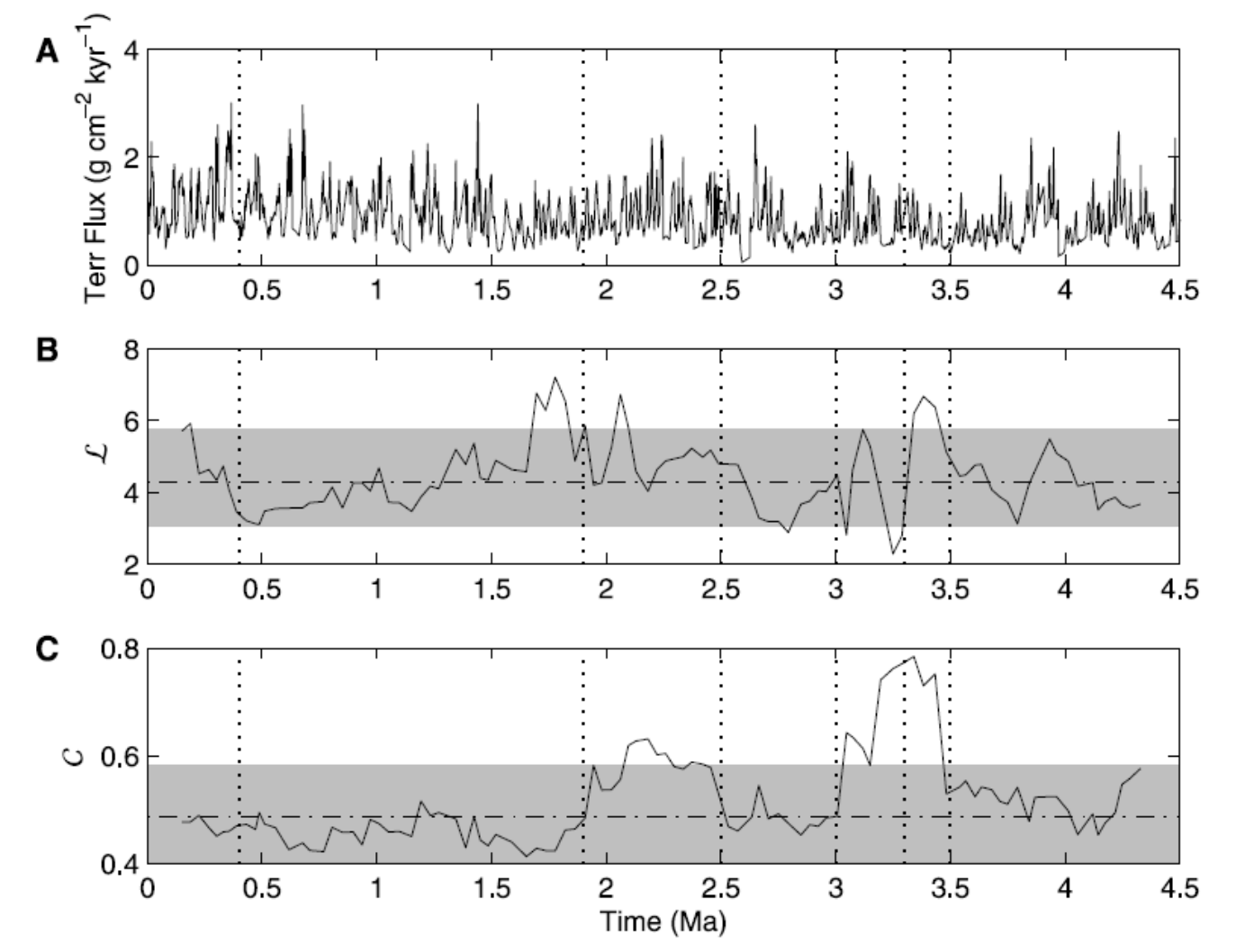

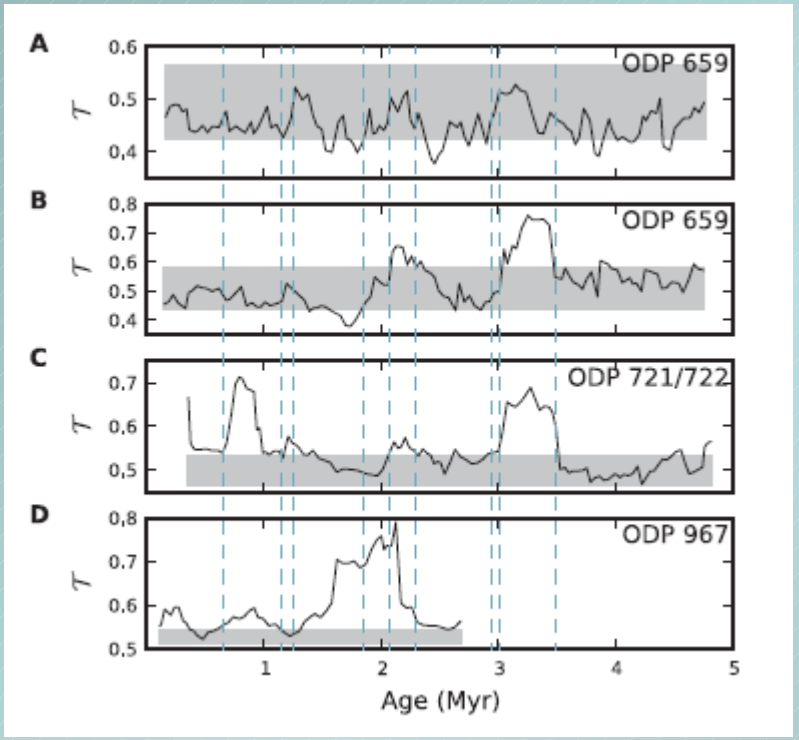

Fig. 9. Evolution of RN transitivity $\mathcal{T}$ for **(A)** the δ^{18}O record from ODP site 659, and the dust flux records from ODP sites **(B)** 659, **(C)** 721, and **(D)** 967. $\mathcal{T}$ reveals changes in the regularity of African climate during the Plio-Pleistocene for the latter three records. Here we used a detrending window size $W_{\mathrm{D}}^{*} = 500$ kyr, recurrence window size $W^{*} = 410$ kyr and step size $\Delta W^{*} = 41$ kyr, embedding dimension $m = 3$ and delay $\tau^{*} = 10$ kyr. The recurrence threshold ε was chosen adaptively to yield a fixed edge density $\rho = 0.05$. The grey bars represent the 5 % and 95 % quantiles with respect to the test distribution obtained from 10 000 realisations of our null-model for each record separately. Vertical dashed lines indicate the detected epochs of transitions discussed in the main text.

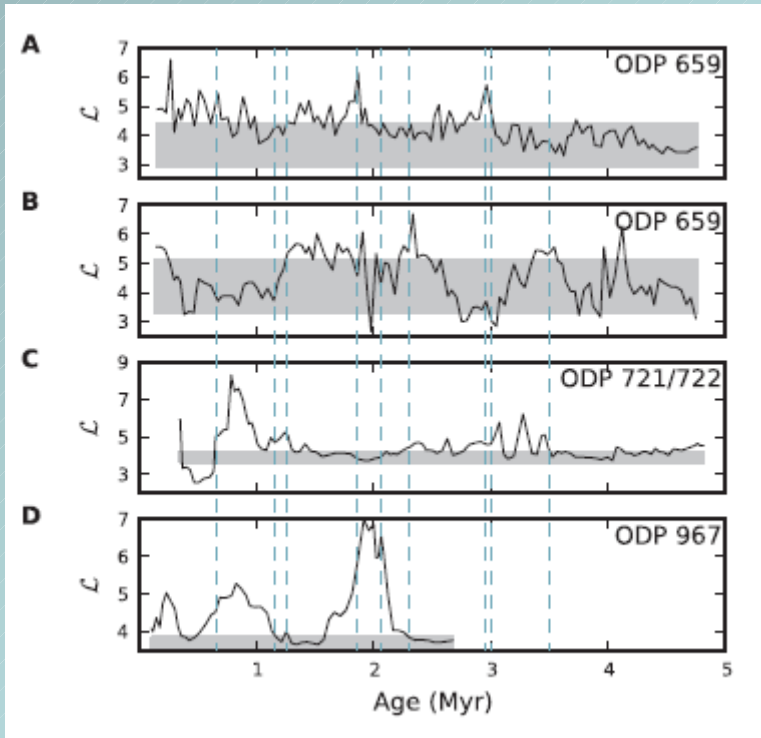

Fig. 10. Evolution of RN average path length $\mathcal{L}$ for **(A)** the $\delta^{18}O$ record from ODP site 659, and the dust flux records from ODP sites **(B)** 659, **(C)** 721, and **(D)** 967, indicating transitions in African climate dynamics during the Plio-Pleistocene. Parameters, significance test, and vertical lines are the same as in Fig. 9.

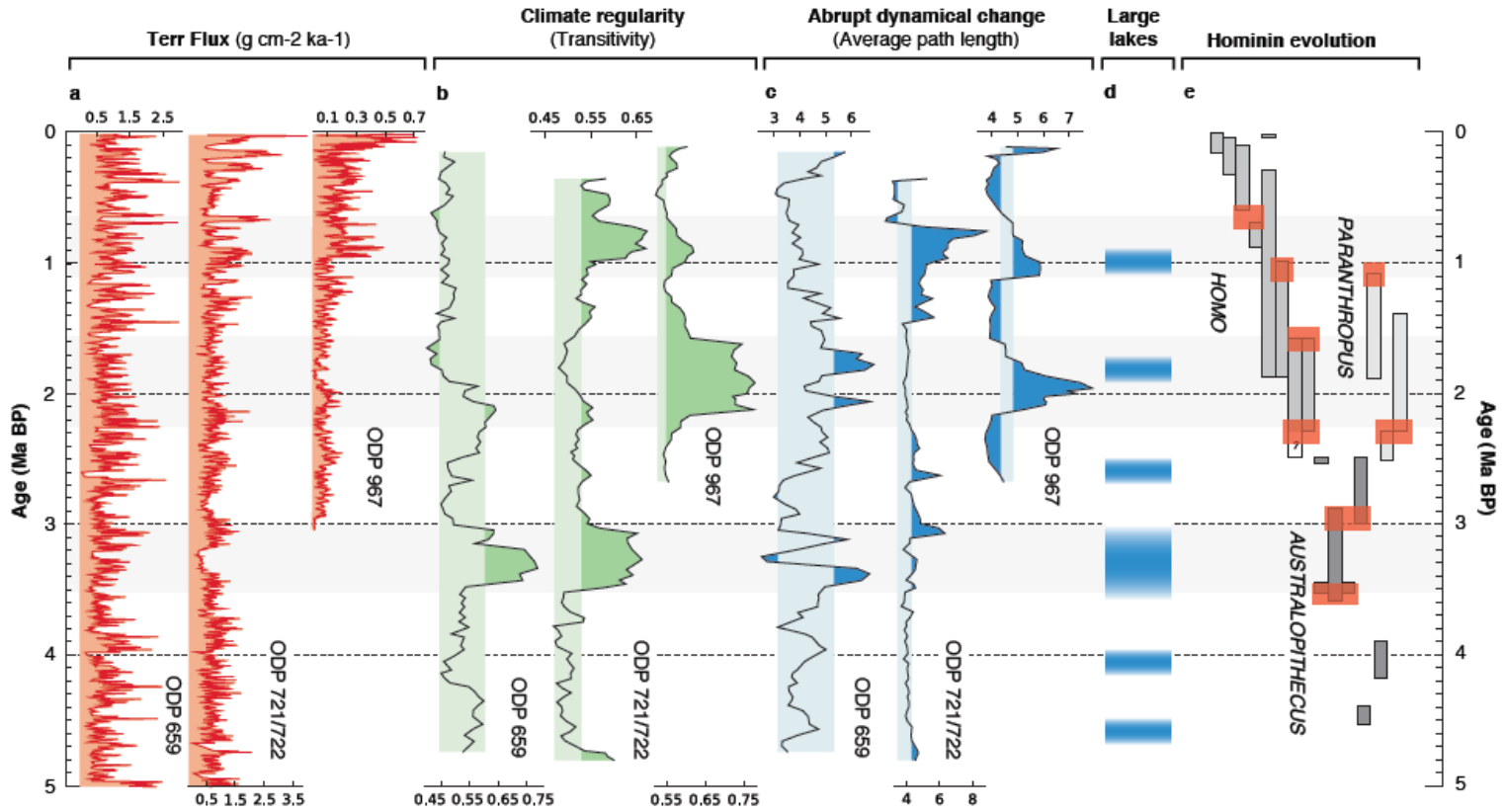

Fig. 2. (a) Terrestrial dust flux records from the three considered ODP sites (1,2,34,66). (b,c) Results of RN analysis of the three dust flux records including 90% confidence bands (vertical shadings) of a stationarity test (SI text). Comparing both measures for all records reveals significant and synchronous large-scale regime shifts in dust flux dynamics (horizontal shadings). (d) Time intervals with geological evidence for large lakes in East Africa, comprising collected information from different areas in the EARS (3) and additional results from the Afar basin (65,70). (e) Major known steps of human evolution in East Africa (simplified from (3)). Red bars indicate epochs where the possible emergence and/or extinction of known hominin species coincides with detected climate transitions (SI text).

PNAS, 2011

Main Results

- Average path length: signif. Max. 3.35-3.1, 2.25-1.6, and 1.1-0.7 Ma BP refer to strong transition epochs (Mid-Pliocene, Early Pleistocene, Mid-Pleistocene resp.)
- Cluster coeff: signif. Max 3.5-3.0 and 2.5-2.0
- In good agreement with transitions in hominin evolution in Africa (appearance and disappearance of hominin species)
  ➔ interrelationships between long-term climate change and hominin evolution

Interpretation

- Strong change around 3.35 Ma BP – unusually cold period prior to Middle Pleistocene warm period
- Causes: closure and re-openings of Panamanian Seaway

  Northward displacement of New Guinea (+)

➔ Less warm equatorial Pacific water pass Indonesian throughflow – cooling Indian Ocean/Arabian Sea

Interpretation

- Transition between 2.25 – 1.6: large-scale changes in atmospheric circulation (shift of Walker circulation)
- Transition 1.1 – 0.7: Middle Pleistocene transition – change from dominant Milankovich cycles (orbital time scales 41 ka ➔ 100 ka)

  fits very well with extinction of Paranthropus

Conclusions

- Recurrence offers important insights into nonlinear systems and promising characteristics for time series analysis
- Combining recurrence with complex networks approach provides another new approach to time series analysis
- It is very successful for rather short data sets (paleo-data)
- This approach is in its infancy and needs much more research

Our papers on recurrence networks

- Phys. Lett. A 373, 4246-4254 (2009)
- Phys. Rev. E 81, 015101R (2010)
- New J. Phys. 12, 033025 (2010)
- Nonlin. Proc. Geophys. 18, 545-562 (2011)
- Int. J. Bif.&Chaos 21, 1019-1046 (2011)
- PNAS 108, 20422-20427 (2011)
- Phys. Rev. E 85, 046105 (2012)